the elastic moduli at zero field and pressure are shown in Fig. 2. Data published by Rosen and Klimker [9] show similar, but significantly different, effects. The differences between Fig. 2 and Rosen's data are primarily in the variation of c_{12}; consequently, the variations of the compressibilities $\beta_{\parallel}$ and $\beta_{\perp}$ with turn angle and structure, that are calculated from the Fig. 2 data, are considerably different than given by Rosen. In the present context, however, there appears no indication that magnetic ordering has any influence on the second order elastic moduli at 298°K.

The magnetic structures in Er are even more complex. The spontaneous ferromagnetic phase, with $T_c = 20$°K, contains a spiral component. The ferromagnetic component transforms to an antiferromagnetic arrangement, between 20 and 53°K, and a modulated moment arrangement between 53 and 80°K. The effects of the ordering on the elastic moduli are shown in Fig. 3. These effects are clearly not evident at 298°K.

The values of the second order elastic stiffness moduli at 298°K are listed in Table 2. We include here the data for Ho as given by Palmer and Lee [8]. Included in Table 2 are the values of the density [18] that are used for computing the moduli. The calculated adiabatic and isothermal bulk moduli, K_s and K_T, and also given and the last column gives the parameters $(\beta_{\parallel}-\beta_{\perp})/\beta_V$ calculated from isothermal values of the compressibilities. The latter parameter is that used for computing equation (3). The variations of the data with increasing atomic number (Gd → Er) are noteworthy. The c/a ratio decreases whereas the density increases because of the so-called lanthanide contraction associated with the addition of electrons to the $4f$ shell. There is

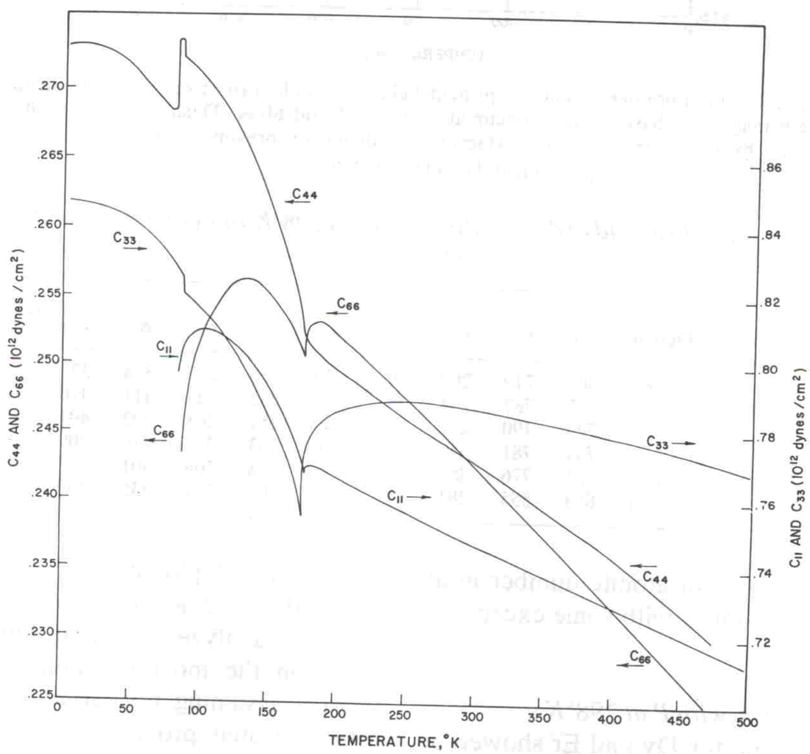

Fig. 2. Temperature dependence of the principal elastic moduli of Dy at zero magnetic field. $T_N = 179$°K and $T_c = 87$°K. Absence of data for c_{11} and c_{66} at $T < 85$°K is result of spontaneous macroscopic distortion by anisotropic magnetostriction.

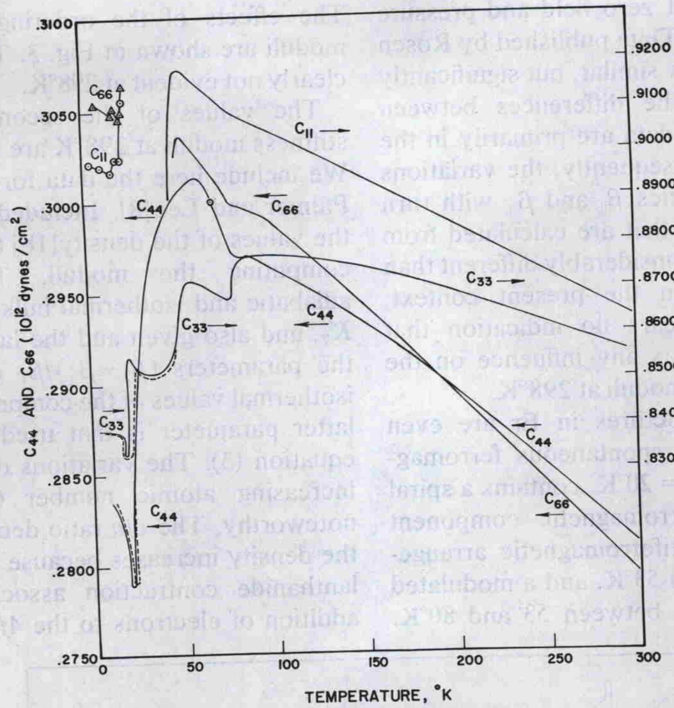

Fig. 3. Temperature dependence of principal elastic moduli in Er at zero magnetic field, where magnetic phase changes occur at ~20, ~53 and 80°K. Dashed lines indicate thermal hysteresis in T_c ~ 20°K. Macroscopic distortion prevented measurements of c_{11} and c_{66} in spiral phase.

Table 2. Values of second order elastic moduli at 298°K of heavy rare earth metals (Kbars)

	c/a	Density	c_{11}	c_{33}	c_{44}	c_{66}	C_H	c_{12}	c_{13}	K_s	K_T	$\left(\frac{\beta_\parallel - \beta_\perp}{\beta_V}\right)_T$
Gd	1·590	7·888	667	719	207	208	250	250	213	378	373	+0·007
Dy(F)	1·573	8·560	747	787	243	243	278	262	223	411	410	−0·005
Dy(R)		8·545	743	790	255	246	290	251	208	402	401	−0·009
Dy(P)		8·560	731	781	240	239	276	253	223	410	409	−0·015
Ho	1·570	8·800	761	776	257	256	290	248	206	401		+0·019
Er	1·569	9·064	863	855	281	279	328	305	227	455	450	+0·043

a general increase with atomic number in all of the c_{ij} and K values, with some exceptions for the Ho data.

(b) *Variations of c_{ij} with P at 298°K*

Plots of the data for Dy and Er showed no significant or systematic departure from linear relations between the c_{ij} and pressure. The Gd data showed small but significant curvature for the c_{33} vs P plot at $P > 2$ Kbar and for c_{44} at $P = 0$ and 2 Kbar. All of the data were, however, analyzed by least square statistics to obtain the most probable values for the dc_{ij}/dP, assuming no curvature. The results with indicated probable errors are given in Table 3. The similarities and differences in the effects of pressure on the c_{ij} of the three metals are evident in the pressure derivatives